A Wideband Full-Duplex Dual-Polarized Antenna with Conical Radiation Pattern

Thu Hang Vu*, Son Xuat Ta*, Thanh Nam Le†, Khac Kiem Nguyen*, Chien Dao-Ngoc*, and Nghia Nguyen-Trong‡
*School of Electronics & Telecommunications, Hanoi University of Science & Technology, Hanoi, 100000, Vietnam
†Information Technology Department, Office of Ministry of Public Security, Hanoi, 100000, Vietnam
‡School of EEE, The University of Adelaide, Adelaide, SA, 5000, Australia
Email: xuat.tason@hust.edu.vn,nghia.nguyentrong@adelaide.edu.au

***Abstract*—This paper presents a wideband dual-polarized antenna with conical radiation pattern for use in in-band full-duplex (IBFD) communications. The design includes a horizontally polarized (HP) dipole array and a vertically polarized (VP) monopole antenna. The dipole array is excited by a feeding network with an in-phase 1:4 power divider to achieve omnidirectional radiation in the horizontal plane. Each HP element is fed by an out-of-phase power divider for improving polarization purity, and consequently, achieving a high isolation. The final design yields an overlapped impedance bandwidth of 48.08% (3.27 – 5.34 GHz), a port-to-port isolation of > 40 dB, and satisfactory conical patterns in both modes. With the features of wideband, conical pattern, high isolation, the proposed antenna is a good candidate for indoor access point in the IBFD systems.**

***Index Terms*—in-band full-duplex, dual-polarization, conical-beam, out-of-phase power divider, polarization purity, high isolation.**

I. Introduction

In-band full-duplex (IBFD) technology [1] has been one of the strongest candidates for the next generation wireless communication systems because of its benefit of potentially doubling the spectrum efficiency relative to the typical frequency/time-division duplex system. A IBFD system, or simultaneous transmission and receiving system, allows transmitting and receiving signals at the same frequency. In order to enable this feature, the IBFD transceiver requires a high isolation of $>$ 100 dB between the Tx and Rx chains. Since no single technology can achieve this required isolation, different isolation techniques are implemented in digital, analog, and antenna stages. Generally, the IBFD antenna requires an isolation of $\geq$ 40 dB [2], which is quite challenging to achieve in a wideband system.

For the application of indoor access points with pervasive coverage, an omnidirectional radiation pattern in the horizontal plane is required. Moreover, dual-polarized antennas are typically adopted due to their features of enhancing spectrum efficiency and mitigating the effects of multipath fading. Accordingly, various dual-polarized omnidirectional antennas have been proposed in literature [3]–[12]. Although, these antennas achieved a wideband operations and dual-polarized omnidirectional radiation, their port-to-port isolation is just 30 dB, which is not suitable for IBFD applications.

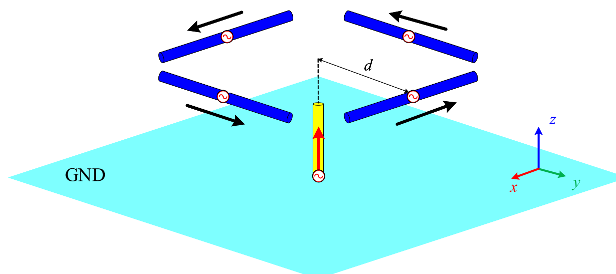

Fig.1. Design concept of the proposed antenna

In this paper, we present a IBFD wideband antenna with high isolation and dual-polarized conical radiation. It is noted that most self-interference cancellation/isolation enhancement techniques were proposed for narrowband system ($<$ 5% bandwidth) [13]–[18]. Wideband IBFD antennas have been proposed but mostly for broadside radiation pattern [19]. The proposed antenna is composed of a dipole array for horizontal polarization (HP) and a monopole antenna for vertical polarization (VP). The two elements are arranged on a planar ground plane for the conical radiation pattern. The dipole array is fed by an in-phase 1:4 power divider to obtain omnidirectional pattern. Each HP element is excited by an out-of-phase power divider [20] to improve polarization purity, and consequently, achieving a high isolation. The antenna system is characterized and optimized using the ANSYS Electronics Desktop.

II. Antenna design and characteristics

A. Design concept

The antenna concept is shown in Fig. 1. The antenna consists of a monopole for VP and four dipoles, which are fed with same magnitude and in phase to achieve the HP conical radiation. Theoretically, if the system is perfectly symmetrical, the isolation between the monopole and the dipole array is infinite. This is because the coupling from the two opposite horizontal dipoles to the monopole are exactly the same in magnitude but opposite in phase. Thus, they perfectly cancel out each other. In practice, the isolation will depend on the feeding network of the horizontal dipole array. A highly

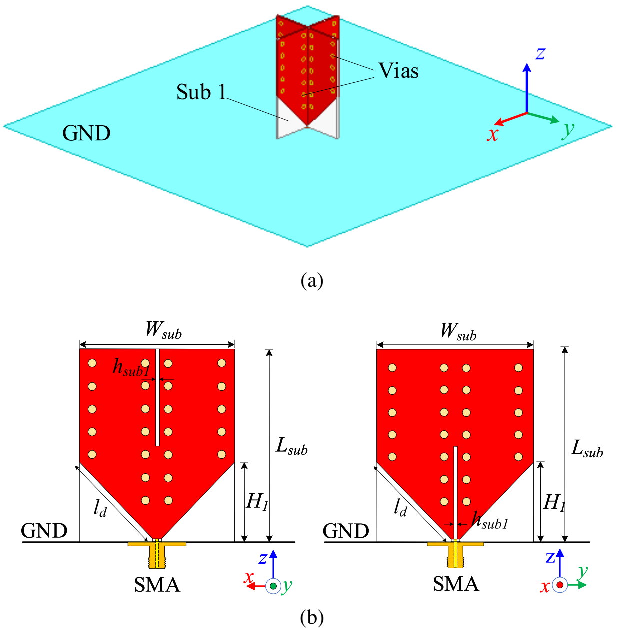

Fig.2. Geometry of the VP element: (a) Perspective view; (b) Front views. The parameters of VP element are W_{sub} = 20, L_{sub} = 25, H_1 = 10, $h_{sub1} = 0.508$.

balanced broadband feed structure is required to achieve the high isolation.

As analyzed using the array factor in [21], the distance d from the center to each horizontal dipole should be less than $0.35\lambda_0$ to achieve a conical omnidirectional pattern with less than 3-dB gain variation in the $\theta_m \approx 45°$-plane. Here, λ_0 is the free-space wavelength at the operating frequency. Thus, we limit the deployment of both HP and VP elements on an area of $0.7\lambda_0 \times 0.7\lambda_0$.

B. VP element

Fig. 2 shows the geometry of the VP element, which is a modified version of a conical monopole design. It is built on two orthogonal Rogers RO4003 substrates ($\varepsilon_r = 3.38$, $\tan\delta = 0.0027$, thickness 0.508 mm) and located at the center of the ground plane. Its primary radiating parts are tapered shapes, which are printed in both sides of the substrates and connected by vias. The antenna is fed by a 50 Ω coaxial line directly; the outer part is connected to the ground plane, whereas the inner pass through the ground plane to connect to the printed monopole.

Fig. 3 shows the characteristics of the VP element. As shown in Fig. 3(a), the antenna yields an ultra-wide bandwidth; its return loss is > 10 dB from 2.21 GHz to excess 10 GHz. As shown in Fig. 3(b), the antenna yields a stable conical radiation pattern across its operational bandwidth.

C. HP element

As mentioned above, the main challenge in realization of the proposed antenna is designing the wideband HP element with nearly perfect balance feed. To address this issue, each dipole of the HP element is fed by the out-of-phase power

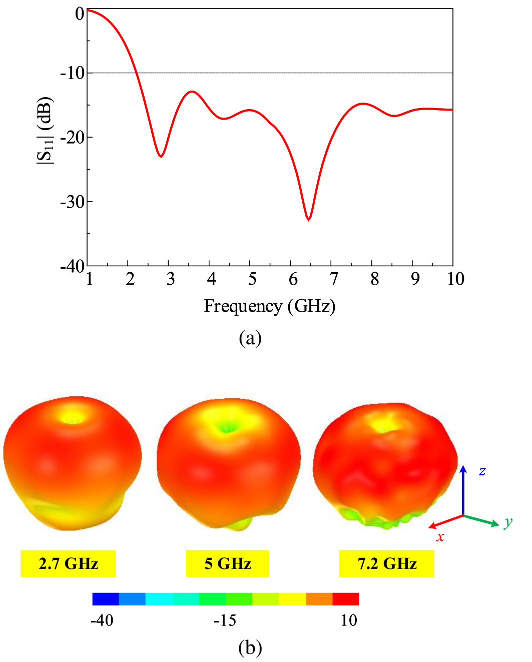

Fig.3. (a) $|S_{11}|$; (b) 3-D total gain radiation patterns of the VP element.

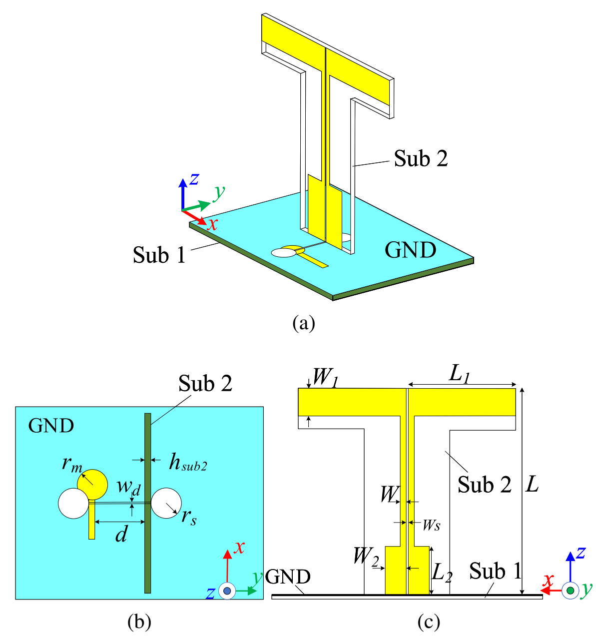

Fig.4. Geometry of the horizontal dipole (a) Perspective view (b) Top view (c) Side view. The design parameters of HP single element are: $w = 0.8$, $w_1 = 4$, $w_2 = 4$, $w_s = 0.3$, $L = 30$, $L_1 = 15.5$, $L_2 = 9$, $w_d = 0.2$, $w_{ms} = 1.1$, $R_s = 1.8$, $R_m = 1.8$, $d = 9$.

divider, as shown in Fig. 4. The power divider is built on both sides of the horizontal substrate (Rogers RO4003 sheet, $\varepsilon_r = 3.38$, $\tan\delta = 0.0027$, and thickness 0.8128 mm), while the dipole is printed on the vertical substrate (Rogers RO4003 sheet, $\varepsilon_r = 3.38$, $\tan\delta = 0.0027$, and thickness 0.8128 mm). The dipole is fed by a coplanar strip-line, which is vertically connected to the outputs of the divider.

The out-of-phase power divider, as shown in Fig. 5(a), is characterized. Based on the analysis in [19], the design is

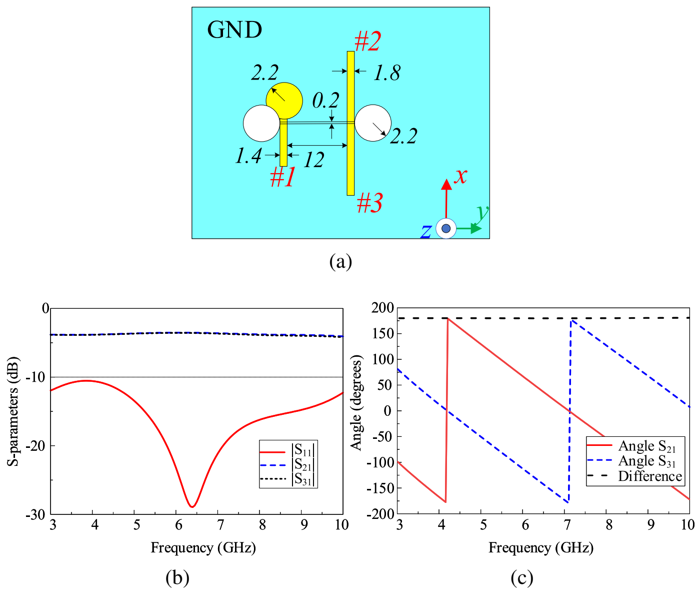

Fig.5. (a) Geometry of the out-of-phase power divider; (b) its S-parameters and (c) Phases.

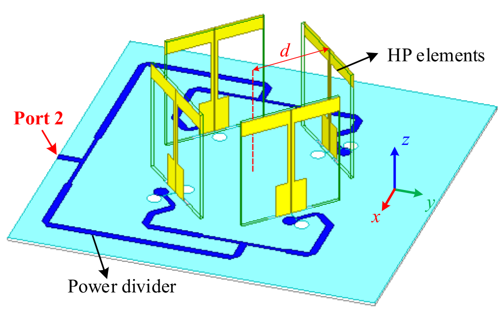

Fig.6. Geometry of the dipoles array antenna.

compensated for the Rogers RO4003 substrate and the lowest operating frequency of 3.0 GHz. Figs. 5(b) and 5(c) show the S-parameters and phase responses of the power divider. It is observed that at the examined frequency range of 3.0 – 10.0 GHz, nearly equal power split and nearly perfect out-of-phase are achieved at the outputs.

Fig. 6 shows the geometry of the HP element, which consists of four dipoles fed by an in-phase 1:4 power divider to obtain the conical radiation pattern. The center-to-center spacing is $2d = 40$ mm, which is less than $0.7\lambda_0$ at the highest frequency. The feeding network is composed of three T-junctions, which is built on a 95×95 mm^2 Rogers RO4003 substrate ($\varepsilon_r = 3.38$, $\tan\delta = 0.0027$, and thickness 0.8128 mm). The feeding network utilizes quarter-wavelength transformers for the impedance matching at the center frequency of 4.0 GHz. As shown in Fig. 7(a), the single dipole and the array design yield a similar bandwidth; their 10-dB return loss bandwidths are 3.27 – 5.34 GHz. From Fig. 7(b), the simulation results indicate that the antenna achieve a stable conical radiation pattern within the operational bandwidth.

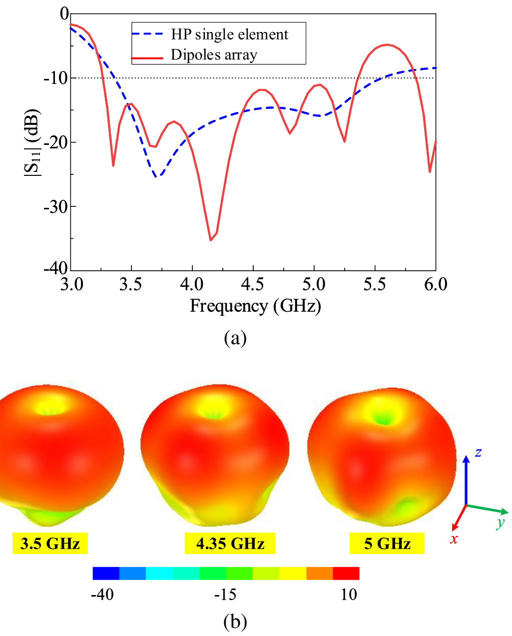

Fig.7. (a) $|S_{11}|$; (b) 3-D total gain radiation pattern of the array dipoles antenna.

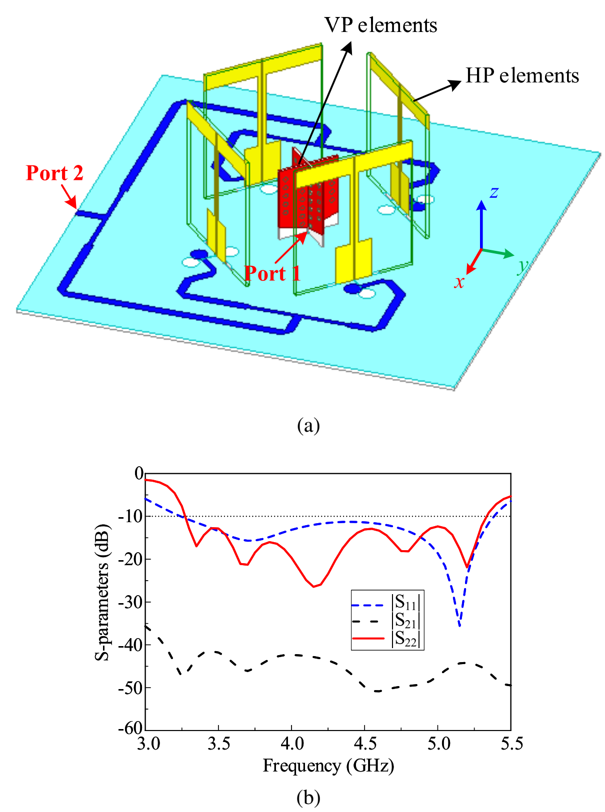

Fig.8. (a) Geometry of the proposed antenna; (b) S-parameters of the design antenna.

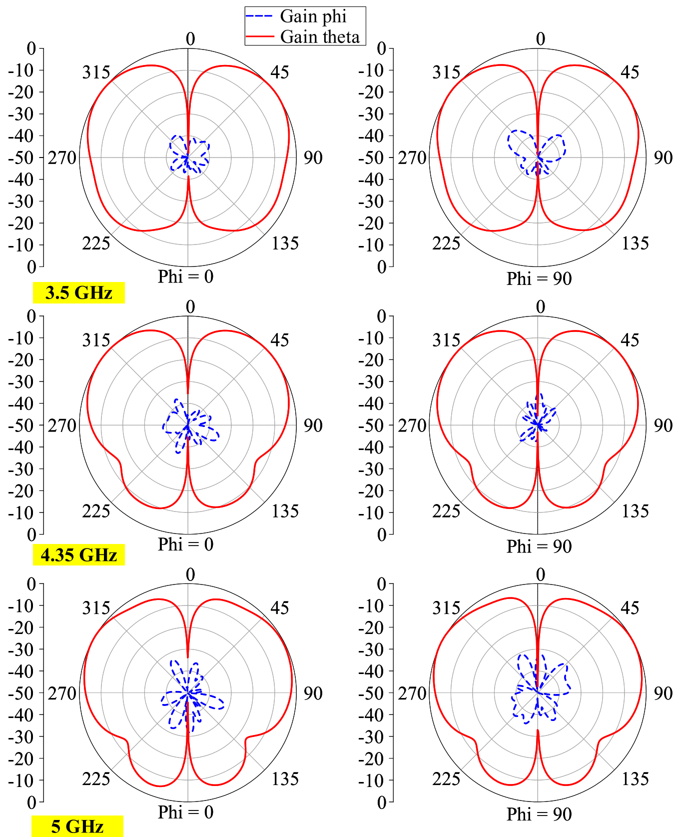

Fig.9. Radiation pattern of the VP element.

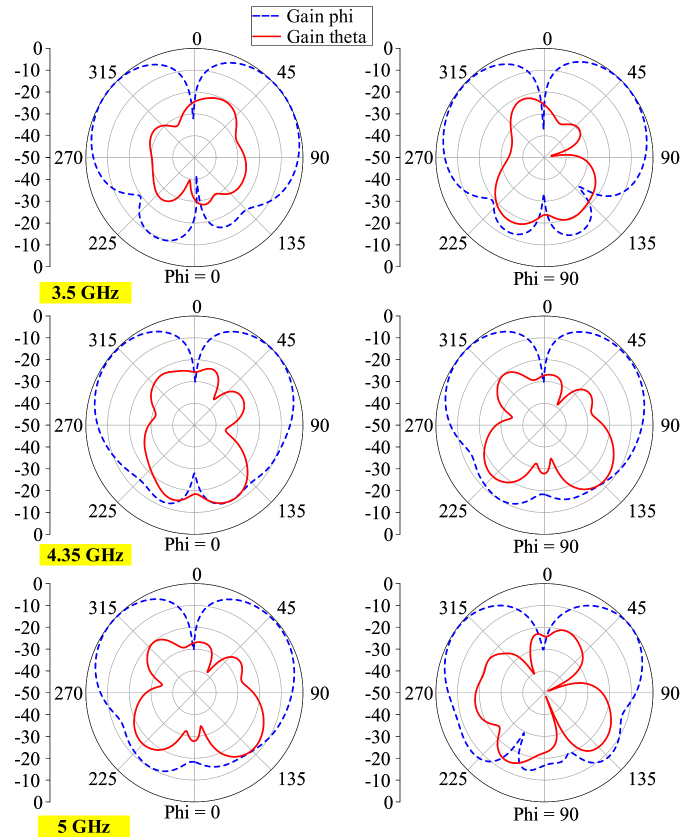

Fig.10. Radiation pattern of the HP element.

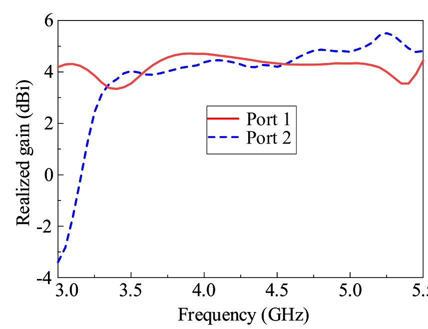

Fig.11. Peak realized gain of the dual-polarized omnidirectional antenna.

D. Dual- polarized full-duplex antenna

Fig. 8(a) shows the geometry of the proposed dual-polarized antenna with conical radiation patterns, which is implemented by the concept in Fig. 1. The proposed antenna is a combination of the VP and HP elements, which are collocated on the common ground plane with size of 95 $\times$ 95 mm^2. Its design parameters are the same as those in Figs. 2 and 6. Fig. 8(b) shows the S-parameters of the dual-polarized antenna. Due to the presence of the HP element, the bandwidth of the VP element is narrowed. Nevertheless, the antenna achieves an overlapped bandwidth of 48.08% (3.27 - 5.34 GHz) for the 10-dB return loss. Also, it yields a port-to-port isolation of $>$ 40 dB, which meets the required value for the IBFD applications.

The radiation patterns of the dual-polarized antenna are shown in Figs. 9 and 10. It is observed that both VP and HP elements achieve a good conical radiation pattern within the wide frequency range. Also, the antenna yields a small cross-polarization level, i.e., < -30 dB for the VP element and < -20 dB for the HP element. Fig. 11 shows the peak gain of the fabricated antenna. Across the overlapped bandwidth, the antenna yields a stable gain of about 4.0 dBi for the VP and HP modes. Moreover, the simulations result in a radiation efficiency of $>$ 90% for the two modes.

III. Conclusion

We have presented a dual-polarized IBFD antenna, which is a combination of a monopole and a HP dipole array for the VP and HP, respectively. The dipole array is excited by a feeding network of in-phase equal 1:4 power divider for the omnidirectional radiation in the horizontal plane. Each dipole of the HP element is fed by an out-of-phase power divider for improving polarization purity, and consequently, achieving a high isolation for the antenna system. The final dual-polarized antenna achieves an overlapped bandwidth of 48.08% (3.27-5.34 GHz), port-to-port isolation of $>$ 40 dB, gain of about 4.0 dB, and radiation efficiency of $>$ 90%. With the features of wideband, high isolation, stable conical radiation pattern, high radiation efficiency, the proposed antenna can be widely used in the IBFD communications. Moreover, it is a good candidate for the indoor access points in the modern wireless communication systems, such as the 5G and beyond.

Acknowledgment

This research is funded by the Hanoi University of Science and Technology (HUST) under project number T2020-SAHEP-016.

References

[1] J. Zhou et al., ”Integrated full duplex radios,” *in IEEE Communications Magazine*, vol. 55, no. 4, pp. 142-151, April 2017.

[2] B. Debaillie et al., ”Analog/RF Solutions Enabling Compact Full-Duplex Radios,” *IEEE Journal on Selected Areas in Communications*, vol. 32, no. 9, pp. 1662-1673, Sept. 2014.

[3] C. Deng, P. Li and W. Cao, ”A High-Isolation Dual-Polarization Patch Antenna With Omnidirectional Radiation Patterns,” *IEEE Antennas and Wireless Propagation Letters*, vol. 11, pp. 1273-1276, 2012.

[4] S. X. Ta, D. M. Nguyen, K. K. Nguyen, C. Dao-Ngoc and N. Nguyen-Trong, ”Dual-Polarized Omnidirectional Antenna with Simple Feed and Ultrawide Bandwidth,” *IEEE Antennas and Wireless Propagation Letters*, vol. 19, no. 5, pp. 871-875, May 2020.

[5] H. Huang, Y. Liu and S. Gong, ”Broadband Dual-Polarized Omnidirectional Antenna for 2G/3G/LTE/WiFi Applications,” *in IEEE Antennas and Wireless Propagation Letters*, vol. 15, pp. 576-579, 2016.

[6] X. Dai, Z. Wang, C. Liang, X. Chen and L. Wang, ”Multiband and Dual-Polarized Omnidirectional Antenna for 2G/3G/LTE Application,” *in IEEE Antennas and Wireless Propagation Letters*, vol. 12, pp. 1492-1495, 2013.

[7] X. W. Dai, G. Q. Luo, Y. H. Qian, X. H. Zhang, H. Y. Jin and Z. C. Hao, ”Dual-Polarized Omnidirectional Antenna With High Isolation Based on the Theory of Characteristic Modes,” *in IEEE Access*, vol. 6, pp. 73416-73422, 2018.

[8] D. Guo, K. He, Y. Zhang and M. Song, ”A Multiband Dual-Polarized Omnidirectional Antenna for Indoor Wireless Communication Systems,” *in IEEE Antennas and Wireless Propagation Letters*, vol. 16, pp. 290-293, 2017.

[9] H. Wen, Y. Qi, Z. Weng, F. Li and J. Fan, ”A Multiband Dual-Polarized Omnidirectional Antenna for 2G/3G/LTE Applications,” *in IEEE Antennas and Wireless Propagation Letters*, vol. 17, no. 2, pp. 180-183, Feb. 2018.

[10] Z. Zhao, J. Lai, B. Feng and C. Sim, ”A Dual-Polarized Dual-Band Antenna with High Gain for 2G/3G/LTE Indoor Communications,” *in IEEE Access*, vol. 6, pp. 61623-61632, 2018.

[11] E. Yetisir, C. Chen and J. L. Volakis, ”Wideband Low Profile Multiport Antenna with Omnidirectional Pattern and High Isolation,” *in IEEE Transactions on Antennas and Propagation*, vol. 64, no. 9, pp. 3777-3786, Sept. 2016.

[12] J. Wu, S. Yang, Y. Chen, S. Qu and Z. Nie, ”A Low Profile Dual-Polarized Wideband Omnidirectional Antenna Based on AMC Reflector,” *in IEEE Transactions on Antennas and Propagation*, vol. 65, no. 1, pp. 368-374, Jan. 2017.

[13] M. Heino, S. Venkatasubramanian, C. Icheln, and K. Haneda, “Design of wavetraps for isolation improvement in compact in-band dull-duplex relay antennas,” *IEEE Transaction on Antennas and Propagation*, vol. 64, no. 3, pp. 1061–1070, Mar. 2016.

[14] X. Wang, W. Che, W. Yang, W. Feng, and L. Gu, “Self-interference cancellation antenna using auxiliary port reflection for full-duplex application,” *IEEE Antennas Wireless Propagation Letters*, vol. 16, pp. 2873–3768, Jul. 2018.

[15] K. Iwanmoto, M. Heino, K. Haneda, and H. Morikawa, “Design of an antenna decoupling structure for an inband full-duplex collinear dipole array,” *IEEE Transaction on Antennas and Propagation*, vol. 66, no. 7, pp. 3763–5579, Oct. 2018.

[16] H. Nawaz and I. Tekin, “Three ports microstrip patch antenna with dual linear and co-polarisation characteristics,” *Electronics Letters*, vol. 53, no. 8, Apr. 2017.

[17] M. S. Amjad, H. Nawaz, K. Ozsoy, O. Gurbuz, and I. Tekin, “A low-complexity full-duplex radio implementation with single antenna,” *IEEE Transaction on Vehicular Technology*, vol. 67, no. 3, pp. 2206 – 2218, Mar. 2018.

[18] C. Goodbody, T. Karacolak, and N. Tran, “A dual-polarized patch antenna for in-band full-duplex applications,” *Electronics Letters*, vol. 54, no. 22, Oct. 2018.

[19] Son Xuat Ta, Nghia Nguyen-Trong, Van Cuong Nguyen, Khac Kiem Nguyen, and Chien Dao-Ngoc, “Broadband dual-polarized antenna using metasurface for full-duplex applications,” *IEEE Antennas and Wireless Propagation Letters*, vol. 20, no. 2, pp. 254 – 258, Feb. 2021.

[20] M. E. Bialkowski and A. M. Abbosh, “Design of a compact UWB outof-phase power divider,” *IEEE Microw. Wireless Compon. Lett.*, vol. 17, no. 4, pp. 289–291, Apr. 2007.

[21] Nghia Nguyen-Trong and Son Xuat Ta, “A wideband monopolar antenna concept and its application to design multi-polarized radiators,” *15th European Conference on Antenna and Propagation (EuCAP)*, 2021.